EARTHQUAKE ENGINEERING AND STRUCTURAL DYNAMICS, VOL. 27, 283–300 (1998)

STRESSES IN LININGS OF BORED TUNNELS

JOSEPH PENZIEN[1]* AND CHING L. WU[2]

[1] *International Civil Engineering Consultants, Inc., Berkeley, CA 94704, U.S.A.*
[2] *Bechtel Corporation, San Francisco, CA 94104, U.S.A.*

SUMMARY

An analytical procedure is presented for evaluating the stresses in linings of bored tunnels caused by kinematic soil–lining interaction. Three cases of plane–strain interaction are treated as produced by (1) relaxation of *in situ* soil stresses near a lining following its installation, (2) overburden pressure at the soil surface, and (3) two-dimensional free-field soil response normal to the lining axis as produced by an earthquake. The procedure is applied separately to a steel lining and a concrete lining for a site located at the lower end of Market Street in San Francisco through which a BART (Bay Area Rapid Transit) tunnel passes. © 1998 John Wiley & Sons, Ltd.

Earthquake Engng. Struct. Dyn., **27**, 283–300 (1998)

KEY WORDS: tunnel linings; tunnel/soil interaction

INTRODUCTION

When boring a cylindrical tunnel through relatively soft soil, a rigid open-face shield (Figure 1) is pressed forward longitudinally (z direction) into the soil, much like the action of a cookie cutter, transferring the *in situ* soil stresses to the outer surface of the shield. As the shield moves forward, a narrow segmental lining ring is installed directly behind the shield and grout is injected between the outer surface of the ring and the inner surface of the cylindrical cavity. It is intended that this grout fill any voids or gaps that may be present. This ring-installation operation is continually repeated as the shield moves forward with the adjacent lining rings being bolted together to secure them in place within the tunnel.

As the shield passes by a fixed point along the longitudinal axis of the tunnel, the soil pressure distribution is transferred to the lining. However, since the lining is quite flexible compared to the shield, the lining will deform under this distribution which, in turn, will modify the pressure distribution. This coupled behaviour of cause and effect is referred to herein as kinematic soil–lining interaction. This same type of interaction will be assumed also for the other two interaction cases mentioned above, namely that produced by overburden pressure at the soil surface and that produced by free-field soil response during an earthquake.

In 1964, Burns and Richard[1] published a paper entitled 'Attenuation of stresses for buried cylinders' which presented a procedure for evaluating the soil–structure interaction behaviour produced by an overburden pressure at the soil surface. The procedure treated the soil surrounding the cylinder as a continuum and derived two-dimensional plane-strain solutions using the Michell series form of the Airy stress function. Later in 1972, Peck *et al.*[2] used these solutions to approximate the stresses in a tunnel lining produced by the relaxation of *in situ* soil stresses near the lining following its installation by the shield tunnelling method. The Michell series form of the Airy stress function was also used by Einstein and Schwartz[3] in 1979 to analyse the linings of tunnels having various support conditions.

* Correspondence to: Joseph Penzien, International Civil Engineering Consultants, Inc., 1995 University Avenue, Suite 119, Berkeley, CA 94704, U.S.A.

CCC 0098–8847/98/030283–18$17·50

Received 27 August 1996
Revised 12 August 1997

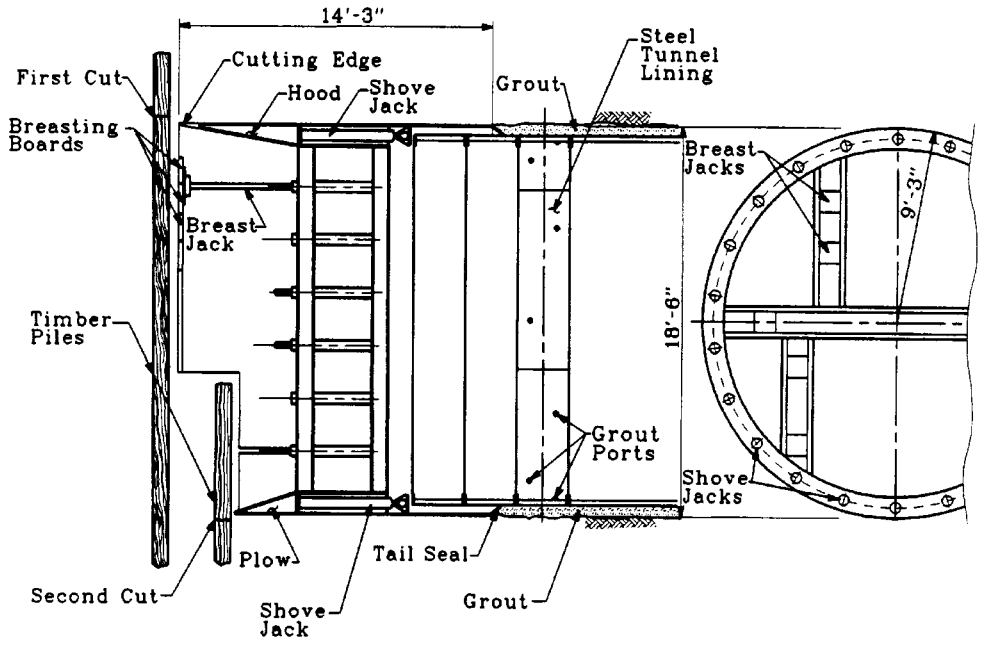

Figure 1. Open face tunnel shield (MUNI Metro Turnback Project, Drawing No. DL-10089)

Because the soil–lining interaction behaviour produced by an applied overburden pressure at the soil surface differs from that behaviour produced by relaxation of the *in situ* soil stresses near a lining following its installation, different solutions should be used to determine these two behaviours. Therefore, this paper presents separate solutions for these two interaction cases using the classical theory of elasticity. In addition, a solution for the case of soil/lining interaction resulting from free-field soil response during an earthquake is presented. Various aspects of global seismic response of linings have been published by Merrit *et al.*[4] in 1985 and by Wang[5] in 1993, which, in particular, evaluate seismic deformation of cross-sections using the formulations of Peck *et al.*[2] with the lateral soil coefficient (K_0) set equal to $-1{\cdot}0$.

In each of the three soil/lining interaction cases mentioned above, subsets of solutions are obtained for two different conditions at the interface between the soil and the lining, namely (1) full continuity of the soil and lining displacements, and (2) full slippage, without normal separation, resulting in no tangential shear forces. The effect of pore pressure due to the presence of ground water is included in the solutions.

The subsequent development of analytical procedures for treating the three cases of soil–lining interaction is separated into four parts (1) *in situ* stress state of the soil through which the tunnel is bored, (2) generalized force/displacement relations of the soil, (3) generalized force/displacement relations of the lining, and (4) soil–lining interactions.

IN SITU STRESS STATE OF SOIL

To assess kinematic soil–lining interaction, the *in situ* stress state of the soil must be known. Consider an infinitesimal element of soil at Pt. *O* as shown in Figure 2, which is located at the origin of coordinate axes x, y and z. The z-axis coincides with the intended longitudinal axis of the tunnel to be bored into the soil as indicated by the dashed circle of diameter D in this figure. The x and y axes will become the transverse and vertical axes of the tunnel cross-section, respectively.

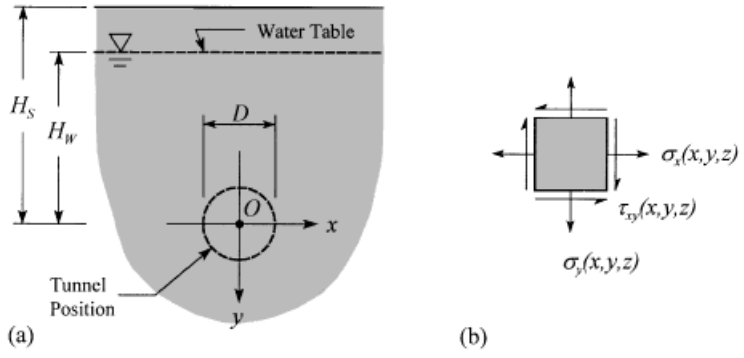

Figure 2. Soil profile and soil element at Pt. *O*

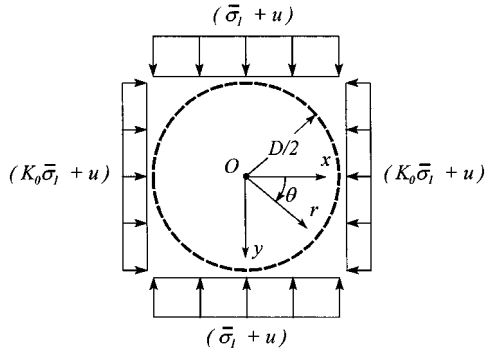

Figure 3. *In situ* soil loading over tunnel height *D*

Planes *xy*, *yx*, and *zy* are principal planes of the element upon which principal normal stresses act as follows:

$$\sigma_y = -\gamma_s H_s = -(\bar{\sigma}_1 + u), \qquad \sigma_x = \sigma_z = -(K_0\bar{\sigma}_1 + u) \tag{1}$$

in which γ_s is the average unit weight of the soil over height H_s, $\bar{\sigma}_1$ is the effective vertical compressive soil stress, u is the pore pressure given by

$$u = \gamma_w H_w \tag{2}$$

and K_0 is the effective lateral soil coefficient, representing the horizontal component of the initial *in situ* stress, which can have a wide range of values depending upon the site conditions (e.g. if the tunnel is bored into overconsolidated clay, the value of K_0 can exceed unity considerably).

For the purpose of analysis, it will be assumed that the tunnel is to be located sufficiently below ground surface so that approximate solutions can be obtained by treating the *in situ* stress state of the soil as being uniform over the vertical-diameter dimension *D* as indicated in Figure 3. In doing so, the loading represented in this figure will be separated into its dilatational and shear-type loadings as shown in Figures 4(a) and 4(b), respectively.

GENERALIZED FORCE/DISPLACEMENT RELATIONS OF THE SOIL OUTSIDE THE TUNNEL

Due to generalized forces on cavity wall

Consider boring a cylindrical tunnel of diameter D into a soil region which is in the *in situ* stress-state condition shown in Figure 3 and assume no lining rings are installed following passage of the shield. As the shield moves forward, the surface of the cylindrical cavity at a particular cross-section will displace inward unless the full *in situ* soil loadings transferred to the shield can somehow be maintained. Since these loadings are not maintained following passage of the shield, the cavity surface will displace inward due to full release of the *in situ* loadings shown in Figure 3 which act in opposite directions on the cavity surface. To calculate the inward displacement due to the release of these loadings, which corresponds to applying the same loadings shown in Figure 3 to the cavity surface, they will be separated into their dilatational and shear-type components. Further, for convenience in analysis, these separate cavity-boundary loadings will be expressed in cylindrical co-ordinates. Doing so for the loadings shown in Figures 4(a) and 4(b), but ignoring the pore pressure u (since its effects will be treated separately later), one obtains,

$$\sigma_r(R,\theta) = \frac{\bar{\sigma}_1}{2}(1 + K_0), \qquad \tau_{r\theta}(R,\theta) = 0 \tag{3}$$

and

$$\sigma_r(R,\theta) = -\frac{\bar{\sigma}_1}{2}(1 - K_0)\cos 2\theta, \qquad \tau_{r\theta}(R,\theta) = \frac{\bar{\sigma}_1}{2}(1 - K_0)\sin 2\theta \tag{4}$$

respectively, which follow the standard Timoshenko sign convention.

Using the cavity loadings expressed by equations (3) and (4), elasticity theory[6] can be used to obtain the stress fields for the region $R \leqslant r < \infty$ and $0 \leqslant \theta \leqslant 2\pi$. The stress field produced by the dilatational loading of equation (3) is

$$\sigma_r(r,\theta) = \frac{R^2\bar{\sigma}_1}{2r^2}(1 + K_0), \qquad \sigma_\theta(r,\theta) = \frac{-R^2\bar{\sigma}_1}{2r^2}(1 + K_0)$$
$$\tau_{r,\theta}(r,\theta) = 0 \tag{5}$$

To obtain the stress fields produced by the cavity-boundary loadings expressed by equations (4), the compatibility equation, which also satisfies equilibrium, namely

$$\left(\frac{\partial^2}{\partial r^2} + \frac{1}{r}\frac{\partial}{\partial r} + \frac{1}{r^2}\frac{\partial^2}{\partial\theta^2}\right)\left(\frac{\partial^2\phi}{\partial r^2} + \frac{1}{r}\frac{\partial\phi}{\partial r} + \frac{1}{r^2}\frac{\partial^2\phi}{\partial\theta^2}\right) = 0 \tag{6}$$

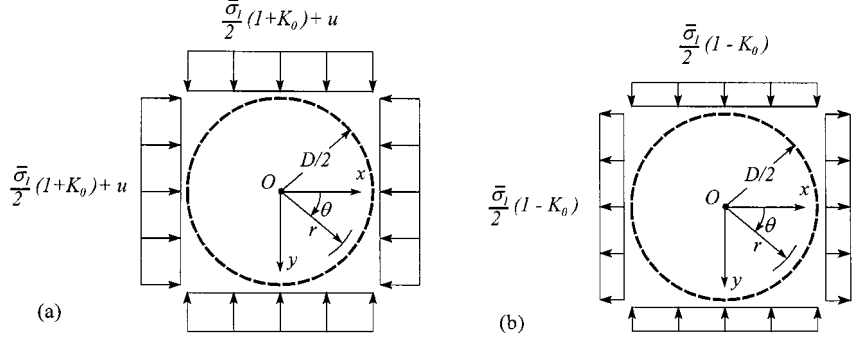

Figure 4. Separation of *in situ* soil loading into its dilatational (a) and shear-type (b) components

must be used, in which the Airy stress function ϕ is of the following form:

$$\phi(r,\theta) = f(r)\cos 2\theta \tag{7}$$

which separates the variables r and θ. Substituting this function into equation (6) yields the ordinary differential equation

$$\left(\frac{\mathrm{d}^2}{\mathrm{d}r^2} + \frac{1}{r}\frac{\mathrm{d}}{\mathrm{d}r} - \frac{4}{r^2}\right)\left(\frac{\mathrm{d}^2 f}{\mathrm{d}r^2} + \frac{1}{r}\frac{\mathrm{d}f}{\mathrm{d}r} - \frac{4}{r^2}\right) = 0 \tag{8}$$

which has the solution

$$f(r) = Ar^2 + Br^4 + C\frac{1}{r^2} + D \tag{9}$$

Equation (7) therefore becomes

$$\phi(r,\theta) = \left(Ar^2 + Br^4 + C\frac{1}{r^2} + D\right)\cos 2\theta \tag{10}$$

Having evaluated the Airy stress function, the stress fields in the region $R \leqslant r < \infty$ and $0 \leqslant \theta < 2\pi$ can be obtained using

$$\begin{gathered}\sigma_r(r,\theta) = \frac{1}{r}\frac{\partial\phi}{\partial r} + \frac{1}{r^2}\frac{\partial^2\phi}{\partial\theta^2}, \qquad \sigma_\theta(r,\theta) = \frac{\partial^2\phi}{\partial r^2} \\ \tau_{r\theta}(r,\theta) = \frac{1}{r^2}\frac{\partial\phi}{\partial\theta} - \frac{1}{r}\frac{\partial^2\phi}{\partial r\,\partial\theta}\end{gathered} \tag{11}$$

Upon substitution of equation (10) into these relations, one obtains

$$\begin{gathered}\sigma_r(r,\theta) = -\left(2A + \frac{6C}{r^4} + \frac{4D}{r^2}\right)\cos 2\theta, \qquad \sigma_\theta(r,\theta) = \left(2A + 12Br^2 + \frac{6C}{r^4}\right)\cos 2\theta \\ \tau_{r\theta}(r,\theta) = \left(2A + 6Br^2 - \frac{6C}{r^4} + \frac{2D}{r^2}\right)\sin 2\theta\end{gathered} \tag{12}$$

The constants A, B, C, and D in these equations can be obtained by satisfying the stress boundary conditions at $r = R$ as expressed by equations (4) and at $r = \infty$ as given by $\sigma_r(\infty,\theta) = 0$ and $\tau_{r\theta}(\infty,\theta) = 0$. To facilitate investigation of normal and tangential interaction between the lining and surrounding soil medium separately, equations (4) are divided into the two sets of two separate cavity-boundary loadings given by

$$\sigma_r(R,\theta) = -\frac{\bar{\sigma}_1}{2}(1 - K_0)\cos 2\theta; \qquad \tau_{r\theta}(R,\theta) = 0$$

and (13)

$$\sigma_r(R,\theta) = 0; \qquad \tau_{r\theta}(R,\theta) = \frac{\bar{\sigma}_1}{2}(1 - K_0)\sin 2\theta$$

The corresponding stress fields given by equations (12) become

$$\begin{gathered}\sigma_r(r,\theta) = -\bar{\sigma}_1(1 - K_0)\left[\left(\frac{R}{r}\right)^2 - \frac{1}{2}\left(\frac{R}{r}\right)^4\right]\cos 2\theta \\ \sigma_r(r,\theta) = -\frac{\bar{\sigma}_1}{2}(1 - K_0)\left(\frac{R}{r}\right)^4\cos 2\theta \\ \tau_{r\theta}(r,\theta) = -\frac{\bar{\sigma}_1}{2}(1 - K_0)\left[\left(\frac{R}{r}\right)^2 - \left(\frac{R}{r}\right)^4\right]\sin 2\theta\end{gathered} \tag{14}$$

and

$$\sigma_r(r,\theta) = -\bar{\sigma}_1(1-K_0)\left[\left(\frac{R}{r}\right)^2 - \left(\frac{R}{r}\right)^4\right]\cos 2\theta$$

$$\sigma_\theta(r,\theta) = -\bar{\sigma}_1(1-K_0)\left(\frac{R}{r}\right)^4\cos 2\theta \tag{15}$$

$$\tau_{r\theta} = \frac{\bar{\sigma}_1}{2}(1-K_0)\left[2\left(\frac{R}{r}\right)^4 - \left(\frac{R}{r}\right)^2\right]\sin 2\theta$$

respectively.

Of interest in the subsequent analytical development is the radial-strain relation $\varepsilon_r(r,\theta)$ for each of the above loading cases, since it is needed to determine the corresponding diameter-change distributions with respect to θ. This relation will now be determined under the condition of plane stress as given by Hooke's law

$$\varepsilon_r(r,\theta) = \frac{1}{E_s}\left[\sigma_r(r,\theta) - \nu_s\sigma_\theta(r,\theta)\right] \tag{16}$$

in which ν_s and E_s represent Poisson's ratio and Young's modulus, respectively, for the soil in its *in situ* state. The resulting diameter-change distributions can then be easily converted to the plane-strain condition ($\varepsilon_z = 0$).

Substituting separately the first two of equations (5), (14), and (15) into equation (16) yields

$$\varepsilon_r^{\mathrm{d}}(r,\theta) = \frac{R^2\bar{\sigma}_1(1+K_0)}{2E_s r^2}(1+\nu_s)$$

$$\varepsilon_r^{\mathrm{sn}}(r,\theta) = -\frac{\bar{\sigma}_1(1-K_0)}{E_s}\left[\left(\frac{R}{r}\right)^2 - \frac{1}{2}(1+\nu_s)\left(\frac{R}{r}\right)^4\right]\cos 2\theta \tag{17}$$

$$\varepsilon_r^{\mathrm{st}}(r,\theta) = -\frac{\bar{\sigma}_1(1-K_0)}{E_s}\left[\left(\frac{R}{r}\right)^2 - (1+\nu_s)\left(\frac{R}{r}\right)^4\right]\cos 2\theta$$

respectively. The superscript d has been added to the strain term $\varepsilon_r(r,\theta)$ above to denote the dilatational loading given by equations (3), while the superscripts sn and st have been added to denote the normal and tangential components of the shear-type loading as expressed by the first and second of equations (13), respectively.

Having the radial strain functions of equations (17), the corresponding diameter-change distributions around the cavity wall can be obtained using

$$\Delta D(\theta) = -2\int_R^\infty \varepsilon_r(r,\theta)\,\mathrm{d}r \tag{18}$$

Substituting separately each of equations (17) into this expression yields

$$\bar{\Delta}D_{\mathrm{ds}}(\theta) = -\frac{R\bar{\sigma}_1}{E_s}(1+K_0)(1+\nu_s)$$

$$\bar{\Delta}D_{\mathrm{ss}}^{\mathrm{sn}}(\theta) = \frac{R\bar{\sigma}_1}{3E_s}(1-K_0)(5-\nu_s)\cos 2\theta \tag{19}$$

$$\bar{\Delta}D_{\mathrm{ss}}^{\mathrm{st}}(\theta) = \frac{2R\bar{\sigma}_1}{3E_s}(1-K_0)(2-\nu_s)\cos 2\theta$$

Adding the last two of these three equations gives the diameter-change distribution resulting from both components, sn and st, of the shear-type loading acting together. Doing this yields

$$\bar{\Delta}D_{ss}(\theta) = \bar{\Delta}D_{ss}^{sn}(\theta) + \bar{\Delta}D_{ss}^{st}(\theta) = \frac{R\bar{\sigma}_1}{E_s}(1 - K_0)(3 - \nu_s)\cos 2\theta \tag{20}$$

The bar has been placed above Δ in equations (19) and (20) to denote the plane-stress condition. These equations can be converted to represent the plane-strain condition by substituting $E_s/(1 - \nu_s^2)$ for E_s and $\nu_s/(1 - \nu_s)$ for ν_s giving

$$\begin{aligned}
\Delta D_{ds}(\theta) &= -\frac{R\bar{\sigma}_1}{E_s}(1 + K_0)(1 + \nu_s) \\
\Delta D_{ss}^{sn}(\theta) &= \frac{R\bar{\sigma}_1}{3E_s}(1 - K_0)(1 + \nu_s)(5 - 6\nu_s)\cos 2\theta \\
\Delta D_{ss}^{st}(\theta) &= \frac{2R\bar{\sigma}_1}{3E_s}(1 - K_0)(1 + \nu_s)(2 - 3\nu_s)\cos 2\theta \\
\Delta D_{ss}(\theta) &= \frac{R\bar{\sigma}_1}{E_s}(1 - K_0)(1 + \nu_s)(3 - 4\nu_s)\cos 2\theta
\end{aligned} \tag{21}$$

Note that $\Delta D_{ds}(\theta) = \bar{\Delta}D_{ds}(\theta)$ because under the dilatational plane-stress loading condition of equation (3), $\sigma_r(r, \theta) = -\sigma_\theta(r, \theta)$ as shown in equation (5); thus $\varepsilon_z(r, \theta) = 0$ which corresponds identically to the plane-strain condition.

Using equations (21), four different generalized stiffness coefficients for the soil can be obtained as follows: (1) a dilatational coefficient k_{ds} defined as that value of loading $\bar{\sigma}_1(1 + K_0)/2$ which will produce the diameter-change distribution $\Delta D_{ds} = -1$, (2) a shear-component coefficient k_{ss}^{sn} defined as that value of $\bar{\sigma}_1(1 - K_0)/2$ which will produce the diameter-change distribution $\Delta D_{ss}^{sn}(\theta) = \cos 2\theta$, (3) a shear-component coefficient k_{ss}^{st} defined as that value of $\bar{\sigma}_1(1 - K_0)/2$ which will produce the diameter-change distribution $\Delta D_{ss}^{st}(\theta) = \cos 2\theta$, and (4) a combined shear-component coefficient k_{ss} defined as that value of $\bar{\sigma}_1(1 - K_0)/2$ which will produce the diameter-change distribution $\Delta D_{ss}(\theta) = \cos 2\theta$. Using these definitions and satisfying equations (21), one obtains

$$k_{ds} = \frac{E_s}{2R(1 + \nu_s)}; \qquad k_{ss}^{sn} = \frac{3E_s}{2R(1 + \nu_s)(5 - 6\nu_s)} \tag{22}$$

$$k_{ss}^{st} = \frac{3E_s}{4R(1 + \nu_s)(2 - 3\nu_s)}; \qquad k_{ss} = \frac{E_s}{2R(1 + \nu_s)(3 - 4\nu_s)} \tag{23}$$

It can be shown that

$$k_{ss} = \frac{k_{ss}^{sn}k_{ss}^{st}}{(k_{ss}^{sn} + k_{ss}^{st})} \tag{24}$$

corresponding to the two stiffnesses k_{ss}^{sn} and k_{ss}^{st} being in series.

Due to an overburden pressure on the soil surface

Consider now the application of an overburden pressure p to the surface of a uniform soil half-space without a tunnel being present. The principal normal stresses produced at Pt. O in Figure 2 by this loading

will be

$$\sigma_y = -p; \qquad \sigma_x = \sigma_z = -\bar{K}_0 p \tag{25}$$

in which

$$\bar{K}_0 = \nu_s/(1-\nu_s) \tag{26}$$

In this case, the lateral pressure coefficient $\bar{K}_0$ is a function of Poisson's ratio, ν_s, only. It does not depend on the degree of consolidation within the soil.

The corresponding loading on the soil within the imaginary dashed circle of diameter D in Figure 2 can be separated into its dilatational and shear-type components in the same way the *in situ* loading of Figure 3 was separated as shown in Figure 4. It is easily determined that the diameter-change distributions of the circle caused by these dilatational and shear-type components are

$$\begin{aligned} \Delta D_{dc}(\theta) &= -\frac{pR}{E_s}(1+\bar{K}_0)(1+\nu_s)(1-2\nu_s) \\ \Delta D_{sc}(\theta) &= \frac{pR}{E_s}(1-\bar{K}_0)(1+\nu_s)\cos 2\theta \end{aligned} \tag{27}$$

respectively. If the soil within the imaginary circle is now removed bringing the boundary normal and shear stresses on the tunnel wall to zero, additional diameter changes will take place. These changes are obtained by dividing the dilatational and shear-type components of loading eliminated by removal of the soil by the corresponding generalized stiffness coefficients given by the first of equations (22) and the second of equations (23), respectively, resulting the diameter-change distributions

$$\begin{aligned} \Delta D_{dt}(\theta) &= -\frac{pR}{E_s}(1+\bar{K}_0)(1+\nu_s) \\ \Delta D_{st}(\theta) &= \frac{pR}{E_s}(1-\bar{K}_0)(1+\nu_s)(3-4\nu_s)\cos 2\theta \end{aligned} \tag{28}$$

The total dilatational diameter-change distribution of the tunnel wall caused by the overburden pressure p is obtained by adding the first of equations (27) to the first of equations (28); and, the total shear-type diameter-change distribution is obtained by adding the second of these two sets of equations.

Doing so, yields

$$\begin{aligned} \bar{\Delta} D_d(\theta) &= -\frac{2pR}{E_s}(1+\bar{K}_0)(1-\nu_s^2) \\ \bar{\Delta} D_s(\theta) &= \frac{4pR}{E_s}(1-\bar{K}_0)(1-\nu_s^2)\cos 2\theta \end{aligned} \tag{29}$$

in which a bar has been added above the terms $\Delta D_d(\theta)$ and $\Delta D_s(\theta)$ to denote the loading case of an overburden pressure p applied to the soil surface.

Due to seismic ground response

Assume the free-field ground response produced during an earthquake is in the transverse direction to the tunnel. From a standard site-response analysis, using the vertically propagating shear-wave model, the distribution of horizontal free-field ground displacement with depth y, $u(y,t)$, is obtained. In this analysis, one finds the critical distribution $u(y,t_c)$ at time t_c which produces the maximum shear-type deformation of the soil over the depth D of the intended tunnel. The function $u(y,t_c)$ will usually be reasonably linear over

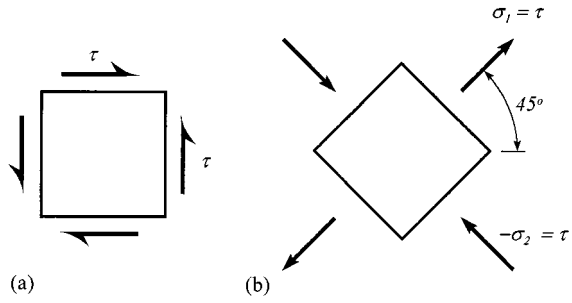

Figure 5. State of stress due to seismic soil response

the range $-D/2 < y < D/2$. In this case, the average free-field shear strain of the soil in the xy plane over this depth is given by the approximate relation

$$\gamma_c = \frac{u(-D/2, t_c) - u(D/2, t_c)}{D} \tag{30}$$

The corresponding state of stress over the depth D is of the shear-type shown in Figure 5(a) which is equivalent to that state of stress shown in Figure 5(b). The individual stresses in this case are given by

$$\tau = \sigma_1 = -\sigma_2 = \frac{\gamma_c \bar{E}_s}{2(1+\bar{\nu}_s)} \tag{31}$$

in which the shear modus $\bar{G}_s$ is equal to $\bar{E}_s/2(1+\bar{\nu}_s)$ and should be assigned a value compatible with the critical shear-strain level γ_c. These stresses will produce an ovalling of the imaginary circle of diameter D shown in Figure 2 with its major and minor axes in the $\pm 45^\circ$ directions as indicated in Figure 5(b). If a tunnel of diameter D is present when the earthquake occurs, its diameter-change distribution in the ovalling mode is obtained by simply substituting $\gamma_c \bar{E}_s/2(1+\bar{\nu}_s)$ for $p(1-\bar{K}_0)/2$ and $\cos 2(\theta + \pi/4)$ for $\cos 2\theta$ in the second of equations (29) resulting in the relation

$$\bar{\bar{\Delta}} D_s(\theta) = 4R\gamma_c(1-\bar{\nu}_s)\cos 2(\theta + \pi/4) \tag{32}$$

in which the double bar over the term $\Delta D_s(\theta)$ denotes the seismic free-field ground response causing the diameter changes.

GENERALIZED FORCE/DISPLACEMENT RELATIONS OF THE LINING

The generalized dilatational stiffness of the lining, defined as that intensity of uniform pressure required on its outer surface to produce an inward diameter-change distribution equal to unity under the plane-strain condition $\varepsilon_z = 0$, is given by

$$k_{d1} = E_1 A_1 / 2R^2(1-\nu_1^2) \tag{33}$$

For the purpose of evaluating generalized stiffnesses of the lining due to shear-type loading as shown in Figure 4(b) of intensity p, this loading will be converted to its equivalent normal and tangential components acting on the outside of the lining as expressed by

$$p_n(R,\theta) = p\cos 2\theta, \qquad p_t(R,\theta) = p\sin 2\theta \tag{34}$$

which will allow separate investigations of the normal and tangential interactions between the lining and the surrounding soil medium.

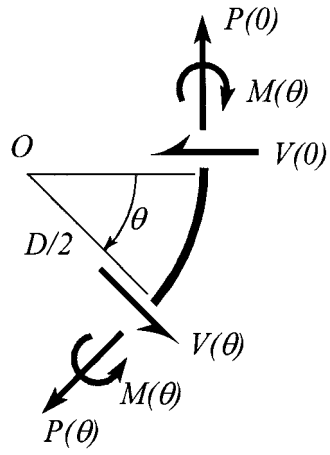

Figure 6. Sign convention for force components in lining

Using the sign convention shown in Figure 6, it can be shown that the distributions of internal axial force, shear, and bending moment per unit of longitudinal (z direction) dimension are given by

$$P_{\mathrm{n}}(\theta) = -\tfrac{1}{3}pR\cos 2\theta, \quad V_{\mathrm{n}}(\theta) = -\tfrac{2}{3}pR\sin 2\theta, \quad M_{\mathrm{n}}(\theta) = -\tfrac{1}{3}pR^2\cos 2\theta \tag{35}$$

when only the loading $p_{\mathrm{n}}(R,\theta)$ is acting on the lining, and by

$$P_{\mathrm{t}}(\theta) = -\tfrac{2}{3}pR\cos 2\theta, \quad V_{\mathrm{t}}(\theta) = -\tfrac{1}{3}pR\sin 2\theta, \quad M_{\mathrm{t}}(\theta) = -\tfrac{1}{6}pR^2\cos 2\theta \tag{36}$$

when only the loading $p_{\mathrm{t}}(R,\theta)$ is acting on the lining. When both loadings $p_{\mathrm{n}}(R,\theta)$ and $p_{\mathrm{t}}(R,\theta)$ are acting together, the distributions are

$$P(\theta) = -pR\cos 2\theta, \quad V(\theta) = -pR\sin 2\theta, \quad M(\theta) = -\tfrac{1}{2}pR^2\cos 2\theta \tag{37}$$

Using the method of virtual work and assuming the plane-strain condition, the diameter changes at $\theta = 0$ and $\theta = \pi/2$ due to loading $p_{\mathrm{n}}(R,\theta)$ and the diameter changes at these same values of θ due to loading $p_{\mathrm{t}}(R,\theta)$ are given by the relations

$$\Delta D_{\mathrm{sl}}^{\mathrm{sn}}(R,0) = -\Delta D_{\mathrm{sl}}^{\mathrm{sn}}(R,\pi/2) = \frac{2pR^4}{9E_1I_1}(1-\nu_1^2)$$

and (38)

$$\Delta D_{\mathrm{sl}}^{\mathrm{st}}(R,0) = -\Delta D_{\mathrm{sl}}^{\mathrm{st}}(R,\pi/2) = \frac{pR^4}{9E_1I_1}(1-\nu_1^2)$$

respectively, in which ν_1, E_1, and I_1 represent the lining's Poisson's ratio, Young's modulus, and its circumferential cross-section moment of inertia per unit of longitudinal dimension. The contributions of axial and shear stresses in the lining to these shear-mode diameter changes have been ignored as they are negligible. Adding equations (38) yield the diameter changes

$$\Delta D_{\mathrm{sl}}(R,0) = -\Delta D_{\mathrm{sl}}(R,\pi/2) = \frac{pR^4}{3E_1I_1}(1-\nu_1^2) \tag{39}$$

due to both loadings $p_{\mathrm{n}}(R,\theta)$ and $p_{\mathrm{t}}(R,\theta)$ acting together.

Generalized stiffness coefficients for the lining in the shear-type modes under the plane-strain condition will now be defined as follows: (1) a shear-component coefficient k_{sl}^{sn} defined as that value of p which will produce the diameter-change $\Delta D_{sl}^{sn}(R,0)$ equal to unity, (2) a shear-component coefficient k_{sl}^{st} defined as that value of p which will produce the diameter change $\Delta D_{sl}^{st}(R,0)$ equal to unity, and (3) a shear-coefficient k_{sl} defined as that value of p which will produce the diameter change $\Delta D_{sl}(R,0)$ equal to unity when both $p_n(R,\theta)$ and $p_t(R,\theta)$ are acting together. Using these definitions and satisfying equations (38) and (39), one obtains the coefficients

$$k_{sl}^{sn} = \frac{9E_1I_1}{2R^4(1-v_1^2)}; \qquad k_{sl}^{st} = \frac{9E_1I_1}{R^4(1-v_1^2)}; \qquad k_{sl} = \frac{3E_1I_1}{R^4(1-v_1^2)} \tag{40}$$

which satisfy the relation

$$k_{sl} = k_{sl}^{sn}k_{sl}^{st}/(k_{sl}^{sn} + k_{sl}^{st}) \tag{41}$$

All of the above generalized stiffness coefficients of the lining will be used in the subsequent soil–lining interaction analyses.

SOIL–LINING INTERACTIONS

For each of the three loading conditions of the soil treated above, namely (a) relaxation of the *in situ* soil stresses at the tunnel wall location, (2) application of an overburden pressure p on the soil surface, and (3) exposure to free-field seismic ground response, dilatational and shear-type diameter changes of the tunnel wall with no lining present have been evaluated for generalized displacement patterns of the soil and generalized stiffness coefficients have been defined for the corresponding generalized soil and lining displacements. This information is sufficient for determining the lining diameter changes which take place due to soil–lining interaction in each loading case.

Due to relaxation of soil stresses following installation of lining

Consider first the case of relaxing the dilatational soil-stresses in an unlined tunnel following passage of the shield. After relaxation of the stresses, the cylindrical cavity will have a diameter equal to $D + \Delta D_{ds}$; thus, in the case when unstressed lining rings of diameter D are installed, the return of pore pressure and the development of soil–lining interaction following construction will impose a uniform pressure at the soil/lining interface causing the lining to deform inward in a dilatational mode with diameter change Δ_{dl} and the surface of the soil cavity to deform outward in a dilatational mode with diameter change Δ_{ds}. The diameter change Δ_{dl} will consist of one part Δ_{dl}^{u} caused by return of the pore pressure u and another part Δ_{dl}^{s} resulting from soil–lining interaction. That part caused by the pore pressure is given by

$$\Delta_{dl}^{u} = u/k_{dl} \tag{42}$$

To satisfy compatibility of the soil lining diameter changes, it is necessary that

$$\Delta_{dl}^{u} + \Delta_{dl}^{s} + \Delta_{ds} = -\Delta D_{ds} \tag{43}$$

in which ΔD_{ds} is given by the first of equations (21). To satisfy equilibrium at the soil/lining interface, it is required that

$$k_{ds}\Delta_{ds} + u = k_{dl}(\Delta_{dl}^{u} + \Delta_{dl}^{s}) \tag{44}$$

Solving equations (42)–(44) simultaneously for Δ_{dl}^{s} yields

$$\Delta_{dl}^{s} = \frac{k_{ds}}{(k_{dl} + k_{ds})}\left[\Delta D_{ds} + \frac{u}{k_{dl}}\right] \tag{45}$$

Substituting the first of equations (21), the first of equations (22), and equation (33) into this equation gives, after some rearrangement of terms, the relation

$$\Delta_{\mathrm{dl}}^{s} = \frac{\bar{\sigma}_1 R(1 + K_0)(1 + \nu_s)}{E_s(1 + \alpha_d)} - \frac{2uR^2(1 - \nu_l^2)}{E_l A_l(1 + \alpha_d)} \tag{46}$$

in which α_d is a dimensionless parameter defined by

$$\alpha_d \equiv E_l A_l(1 + \nu_s)/RE_s(1 - \nu_l^2) \tag{47}$$

Substituting equation (33) into equation (42) yields

$$\Delta_{\mathrm{dl}}^{u} = \frac{2uR^2(1 - \nu_l^2)}{E_l A_l} \tag{48}$$

Adding equations (46) and (48) expresses the total inward diameter change of the lining, which can be simplified to the form

$$\Delta_{\mathrm{dl}} = \frac{\bar{\sigma}_1 R(1 + K_0)(1 + \nu_s)}{E_s(1 + \alpha_d)} + \frac{2uR^2(1 - \nu_l^2)\alpha_d}{E_l A_l(1 + \alpha_d)} \tag{49}$$

Equations identical in form to equation (45), but with its pore pressure term u/k_{dl} removed, can be used to obtain the diameter changes of the lining due to shear-type soil–lining interactions. If this type of interaction takes place with full continuity of the soil and lining displacements at the soil/lining interface, then by substituting the fourth of equations (21), the second of equations (23), and the third of equations (40) into equation (45), with the term u/k_{dl} removed, one obtains

$$\Delta_{\mathrm{sl}} = \frac{\bar{\sigma}_1 R(1 - K_0)(1 + \nu_s)(3 - 4\nu_s)}{E_s(1 + \alpha_s)} \cos 2\theta \tag{50}$$

in which

$$\alpha_s = \frac{6E_l I_l(1 + \nu_s)(3 - 4\nu_s)}{R^3 E_s(1 - \nu_l^2)} \tag{51}$$

If the interaction takes place with full slippage at the interface, without normal separation, resulting in no tangential shear forces, then by substituting the fourth of equations (21), the second of equations (22), and the first of equations (40) into equation (45), again with the term u/k_{dl} removed, yields

$$\Delta_{\mathrm{sl}}^{\mathrm{sn}} = \frac{\bar{\sigma}_1 R(1 - K_0)(1 + \nu_s)(3 - 4\nu_s)}{E_s(1 + \alpha_s^{\mathrm{sn}})} \cos 2\theta \tag{52}$$

in which

$$\alpha_s^{\mathrm{sn}} = \frac{3E_l I_l(1 + \nu_s)(5 - 6\nu_s)}{R^3 E_s(1 - \nu_l^2)} \tag{53}$$

Due to an overburden pressure on the soil surface

Equation (45), again modified with the term u/k_{dl} removed, can be used to obtain the diameter changes of the lining due to an overburden pressure p being applied to the soil surface. Substituting the first of equations (22), the first of equations (29), and equation (33) into this modified form of equation (45), one obtains the dilatational inward diameter change

$$\bar{\Delta}_{\mathrm{dl}} = \frac{2pR(1 + \bar{K}_0)(1 - \nu_s^2)}{E_s(1 + \alpha_d)} \tag{54}$$

in which α_d is defined by equation (47); substituting the second of equations (23), the second of equations (29), and the third of equations (40), into the modified form of equation (45) yields, for the case of full continuity of the soil and lining displacements at the soil/lining interface,

$$\bar{\Delta}_{sl} = \frac{2pR(1-\bar{K}_0)(1-\nu_s^2)}{E_s(1+\alpha_s)} \cos 2\theta \tag{55}$$

in which α_s is defined by equation (51); and finally, substituting the second of equations (22), the second of equations (29), and the first of equations (40) into the modified form of equation (45) gives, for the case of full range slippage at the soil/lining interface,

$$\bar{\Delta}_{sl}^{sn} = \frac{4pR(1-\bar{K}_0)(1-\nu_s^2)}{E_s(1+\alpha_s^{sn})} \cos 2\theta \tag{56}$$

in which α_s^{sn} is defined by equation (53). A bar has been placed above the terms Δ_{dl}, Δ_{sl}, and Δ_{sl}^{sn} in equations (54), (55), and (56), respectively, to denote the loading case of an overburden pressure p applied to the soil surface.

Due to seismic ground response

Again using the modified form of equation (45), in the same way equations (55) and (56) were obtained but using the unlined tunnel diameter-change distribution given by equation (32), one obtains

$$\begin{aligned} \bar{\bar{\Delta}}_{sl} &= \frac{4R\gamma_c(1-\bar{\nu}_s)}{(1+\alpha_s)} \cos 2\left(\theta + \frac{\pi}{4}\right) \\ \bar{\bar{\Delta}}_{sl}^{sn} &= \frac{4R\gamma_c(1-\bar{\nu}_s)}{(1+\alpha_s^{sn})} \cos 2\left(\theta + \frac{\pi}{4}\right) \end{aligned} \tag{57}$$

The double bars above the terms Δ_{sl} and Δ_{sl}^{sn} denote seismic ground motion response as the source of loading on the lining.

FORCE COMPONENTS IN TUNNEL LINING

Adopting the sign convention shown in Figure 6 for the internal force components $P(\theta)$, $M(\theta)$, and $V(\theta)$, one can establish for the dilatational displacement mode:

$$P_d = -\frac{E_l A_l \Delta_{dl}}{2R(1-\nu_l^2)}, \qquad M_d(\theta) = V(\theta) = 0 \tag{58}$$

Substituting into the first of equations (58) the values of Δ_{dl} given by equations (49) and (54) yields the values of P_d for the stress-relaxation and overburden-pressure cases of loading, respectively.

For the shear-type displacement modes, one can use equations (37) and (39) to obtain

$$P_s(\theta) = -\frac{3E_l I_l \Delta_{sl}}{R^3(1-\nu_l^2)} \cos 2\theta, \quad M_s(\theta) = -\frac{3E_l I_l \Delta_{sl}}{2R^2(1-\nu_l^2)} \cos 2\theta, \quad V_s(\theta) = -\frac{3E_l I_l \Delta_{sl}}{R^3(1-\nu_l^2)} \sin 2\theta \tag{59}$$

and equations (35) and the first of equations (38) to obtain

$$P_{sn}(\theta) = -\frac{3E_l I_l \Delta_{sl}^{sn}}{2R^3(1-\nu_l^2)} \cos 2\theta, \quad M_{sn}(\theta) = -\frac{3E_l I_l \Delta_{sl}^{sn}}{2R^2(1-\nu_l^2)} \cos 2\theta, \quad V_{sn}(\theta) = -\frac{3E_l I_l \Delta_{sl}^{sn}}{R^3(1-\nu_l^2)} \sin 2\theta \tag{60}$$

which represent the case of full continuity of the soil and lining displacements at the soil/lining interface and the case of full slippage at the soil/lining interface, respectively. Substitution of the values of Δ_{sl} and Δ_{sl}^{sn} given

by equations (50) and (52) into the above equations (59) and (60), respectively, will yield results for the stress-relaxation case of loading and substitution of the values $\bar{\Delta}_{sl}$ and $\bar{\Delta}_{sl}^{sn}$ given by equations (55) and (56) will yield the corresponding results for the overburden-pressure case of loading. Equations (59) and (60) can also be used for the seismic loading case by substituting the double-bar values of equations (57) for Δ_{sl} and Δ_{sl}^{sn} and by substituting $(\theta + \pi/4)$ for all values of θ.

Direct superposition can be used to find the combined internal force components for any two, or all three, of the loading cases treated above. In doing so, it is helpful to recognize that, when combining the internal force components due to seismic loading with those of the other two loadings, the following identity can be used:

$$A\cos 2\theta + B\cos 2\theta = \sqrt{A^2 + B^2}\cos 2(\theta + \lambda) \tag{61}$$

in which

$$\lambda = \tfrac{1}{2}\tan^{-1}(B/A) \tag{62}$$

APPLICATION OF THEORY

The previously developed theory will now be applied to two cases involving a steel lining and a concrete lining. Both case studies have been carried out for a site located at the lower end of Market Street in San Francisco where a BART (Bay Area Rapid Transit) tunnel passes through soft soil material (Recent Bay Mud). The conditions at this site as represented in Figure 1 are the following:

$$\begin{gathered} E_s = 14{\cdot}36 \times 10^6 \text{ N/m}^2 \text{ (300 k/ft}^2\text{)}; \qquad K_0 = 0{\cdot}65; \qquad \upsilon_s = 0{\cdot}394 \\ \gamma_s = 17{\cdot}28 \times 10^3 \text{ N/m}^3 \text{ (0{\cdot}110 k/ft}^3\text{)}; \qquad H_s = 16{\cdot}31 \text{ m (53{\cdot}5 ft)} \\ \gamma_w = 9{\cdot}80 \times 10^3 \text{ N/m}^3 \text{ (0{\cdot}0624 k/ft}^3\text{)}; \qquad H_w = 13{\cdot}26 \text{ m; (43{\cdot}5 ft)} \end{gathered} \tag{63}$$

The soil properties vary considerably at this site so the above numerical values for E_s, K_0, and υ_s represent mean levels.

Case 1: Steel lining

The steel lining consists of segmental rings (six segments per ring) having the cross-section shown in Figure 7. The properties of this lining are

$$\begin{gathered} D = 5{\cdot}49 \text{ m (18 ft)}; \quad E_l = 2{\cdot}04 \times 10^{11} \text{ N/m}^2 \text{ (29{\cdot}6} \times 10^6 \text{ psi)}; \; \upsilon_l = 0{\cdot}3 \\ I_l = 9{\cdot}63 \times 10^{-5} \text{ m}^4\text{/m (5{\cdot}87 in}^4\text{/in)}; \quad A_l = 0{\cdot}0314 \text{ m}^2\text{/m (1{\cdot}236 in}^2\text{/in)} \end{gathered} \tag{64}$$

First, let us assume the case of no slippage between the tunnel lining and its surrounding soil. Then, using the above lining properties along with those given for the soil previously and introducing their values appropriately into equations (47), (51), (49), (50), (58), and (59), one obtains

$$\begin{gathered} \alpha_d = 249; \quad \alpha_s = 0{\cdot}886; \quad \Delta_{dl} = 0{\cdot}54 \text{ mm (0{\cdot}0213 in)}; \quad \Delta_{sl} = 10{\cdot}8 \text{ mm (0{\cdot}425 in)} \\ P_d(\theta) = -69{\cdot}8 \times 10^4 \text{ N/m } (-47{\cdot}8 \text{ k/ft}); \quad P_s(\theta = 0) = -3{\cdot}39 \times 10^4 \text{ N/m } (-2{\cdot}32 \text{ k/ft}) \\ M_s(\theta = 0) = -46{\cdot}5 \times 10^3 \text{ Nm/m } (-10{\cdot}4 \text{ k ft/ft}) \end{gathered} \tag{65}$$

As indicated directly below, the maximum deformation and forces in the tunnel lining, particularly the bending moment, due to relaxation of the *in situ* soil stresses are significantly smaller than those obtained by

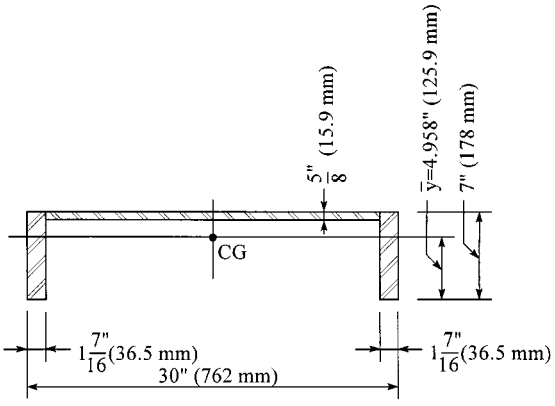

Figure 7. Cross-section of steel lining ring

the formulations provided in Reference 2 (with correction for the effects of pore pressure on the hoop stress and using the condition of no slippage between the lining and soil):

	By stress relaxation	*By overburden pressure* (*Reference* 2)
Max. bending moment	$46{\cdot}5 \times 10^3$ Nm/m (10·4 k ft/ft)	$81{\cdot}82 \times 10^3$ Nm/m (18·39 k ft/ft)
Max. thrust	$73{\cdot}2 \times 10^4$ N/m (50·10 k/ft)	83·10 N/m (56·94 k/ft)
Max. diameter change	11·4 mm (0·446 in)	19·53 mm (0·769 in)

At the above-mentioned BART tunnel site, it has been estimated that the average free-field soil shear strain γ_c could reach the level 0·0028 under maximum credible earthquake conditions (Reference 8). Making use of this value, equations (57) and (59) yield

$$\Delta_{sl} = 9{\cdot}98 \text{ mm } (0{\cdot}392 \text{ in}); \qquad P_s(\theta = -\pi/4) = -3{\cdot}13 \times 10^4 \text{ N/m } (-2{\cdot}14 \text{ k/ft})$$
$$M_s(\theta = -\pi/4) = 42{\cdot}9 \times 10^3 \text{ Nm/m } (-9{\cdot}64 \text{ k ft/ft}) \tag{66}$$

The maximum combined force components in the ovalling mode, when combining the above stress-relaxation and seismic values in accordance with equation (61), are the following:

$$P_s(0^\circ + \lambda) = -[(3{\cdot}39)^2 + (3{\cdot}13)^2]^{1/2} 10^4 = -4{\cdot}61 \times 10^4 \text{ N/m } (-3{\cdot}16 \text{ k/ft})$$
$$M_s(0^\circ + \lambda) = -[(46{\cdot}5)^2 + (42{\cdot}9)^2]^{1/2} 10^3 = -63{\cdot}3 \times 10^3 \text{ Nm/m } (-14{\cdot}2 \text{ k/ft}) \tag{67}$$

The corresponding value of λ is $(1/2)\tan^{-1}(3{\cdot}13/3{\cdot}39) = 21{\cdot}4^\circ$. Adding $P_s(-21{\cdot}4^\circ)$ to $P_d(\theta)$ gives the total combined axial force at $\theta = -21{\cdot}4^\circ$ equal to $-74{\cdot}4 \times 10^4$ N/m ($-51{\cdot}0$ k/ft) where the moment equals $-63{\cdot}3 \times 10^3$ Nm/m ($-14{\cdot}2$ k ft/ft). Combining the resulting circumferential normal stresses produced by these components, one obtains for the cross-section properties and dimensions shown in Figure 7

$$\sigma_o(\theta = -21{\cdot}4^\circ) = +10{\cdot}5 \times 10^6 \text{ N/m}^2 \ (+1508 \text{ psi})$$
$$\sigma_i(\theta = -21{\cdot}4^\circ) = -106{\cdot}4 \times 10^6 \text{ N/m}^2 \ (-15\,433 \text{ psi}) \tag{68}$$

at the outer and inner faces of the lining, respectively.

At $\theta = (-90^\circ - 21{\cdot}4^\circ)$, $P_s(-111{\cdot}4^\circ) = +4{\cdot}61 \times 10^4$ N/m $(+3{\cdot}16$ k/ft) and $M_s(-111{\cdot}4^\circ) = +63{\cdot}3 \times 10^3$ Nm/m $(+14{\cdot}3$ k/ft). Combining the normal stresses produced by $[P_s(-111{\cdot}4^\circ) + P_d(\theta)]$ and M_s $(-111{\cdot}4^\circ)$, one obtains

$$\begin{aligned} \sigma_o(\theta = -111{\cdot}4^\circ) &= -54{\cdot}9 \times 10^6 \text{ N/m}^2 \ (-7951 \text{ psi}) \\ \sigma_i(\theta = -111{\cdot}4^\circ) &= +61{\cdot}0 \times 10^6 \text{ N/m}^2 \ (+8991 \text{ psi}) \end{aligned} \tag{69}$$

at the outer and inner faces, respectively. The maximum compressive stress $(-106{\cdot}4 \times 10^6$ N/m$^2)$ and the maximum tensile stress $(+61{\cdot}0 \times 10^6$ N/m$^2)$ are approximately 43 and 25 per cent of the linings yield stress $(+249 \times 10^6$ N/m$^2)$, respectively.

Let us now consider the case of full slippage between the tunnel and surrounding soil. Using the appropriate formulas for the full-slippage case contained in this paper and repeating the same calculations as for the no-slippage case, the combined normal stresses at the outer and inner fibres of the lining are found to be:

$$\sigma_o(\theta = -21{\cdot}4^\circ) = +12{\cdot}3 \times 10^6 \text{ N/m}^2 \ (+1787 \text{ psi})$$

$$\sigma_i(\theta = -21{\cdot}4^\circ) = -108{\cdot}8 \times 10^6 \text{ N/m}^2 \ (-15\,760 \text{ psi})$$

$$\sigma_o(\theta = -111{\cdot}4^\circ) = -56{\cdot}8 \times 10^6 \text{ N/m}^2 \ (-8230 \text{ psi})$$

$$\sigma_i(\theta = -111{\cdot}4^\circ) = +64{\cdot}3 \times 10^6 \text{ N/m}^2 \ (+9318 \text{ psi})$$

The effect of full slippage increases the bending moment and diameter change by approximately 4 per cent and reduces the thrust by approximately 4 per cent. The maximum tensile and compressive stresses in the lining are increased by approximately 4 and 2 per cent, respectively.

From the above results, it is quite clear that the BART steel lining would perform quite satisfactory under the above combined static and seismic loading conditions.

Case 2: Concrete lining

Consider a concrete lining of diameter $D = 5{\cdot}49$ m (18 ft) and of thickness $t = 0{\cdot}305$ m (1 ft) having a compressive strength $f'_c = 34{\cdot}47 \times 10^6$ N/m^2 (5000 psi), a Young's modulus $E_l = 27{\cdot}77 \times 10^9$ N/m^2 $(0{\cdot}58 \times 10^6$ k/ft$^2)$, and a Possion's ratio $\nu_l = 0{\cdot}17$.

Carrying out the same evaluations described above for discrete values of thickness t, the stresses in the inner fibres at the critical locations $\theta = -\lambda$ and $\theta = (-90^\circ - \lambda)$ can be obtained as functions of lining thickness. These functions are shown in Figure 8 over the thickness range $0 < t < 0{\cdot}61$ m (2 ft). For $t = 0{\cdot}305$ m (1 ft), the maximum combined compressive stress at $\theta = -\lambda$ equals $-8{\cdot}96 \times 10^6$ N/m^2 $(-1298$ psi), of which $-6{\cdot}43 \times 10^6$ N/m^2 $(-932$ psi) and $-2{\cdot}53 \times 10^6$ N/m^2 $(-367$ psi) are produced by deformations in the ovalling and dilatational modes, respectively. For this same thickness, the maximum combined tensile stress at $\theta = (-\lambda - 90^\circ)$ equals $+4{\cdot}37 \times 10^6$ N/m^2 $(+634$ psi), of which $+6{\cdot}43 \times 10^6$ N/m^2 $(+932$ psi) and $-2{\cdot}05 \times 10^6$ N/m^2 $(-298$ psi) are produced by deformations in the ovalling and dilatational modes, respectively. The maximum compressive stress $(-8{\cdot}96 \times 10^6$ N/m^2 $(-1298$ psi)) is well below $f'_c = 34{\cdot}47 \times 10^6$ N/m^2 $(-5000$ psi); however, the maximum tensile stress $(+4{\cdot}37 \times 10^6$ N/m^2 $(+634$ psi)) exceeds the tensile strength of the concrete by about 30 per cent. As shown by Pt. A on the upper curve, a thickness of 0·366 m (1·2 ft) is required to reduce the maximum tensile stress to $3{\cdot}45 \times 10^6$ N/m^2 (500 psi) corresponding to the tensile strength of the concrete. As seen in Figure 8 for a given concrete lining thickness, the maximum normal stresses at the outer and inner fibres of the lining are up to 12 per cent higher for the full-slippage case than for the no-slippage case.

For a thickness in the approximate range 0·1 m (0·328 ft) $< t <$ 0·214 m (0·7 ft), a small increase in its value results in increasing the critical tension stress; while, for a thickness $t >$ 0·214 m (0·7 ft), an increase in its

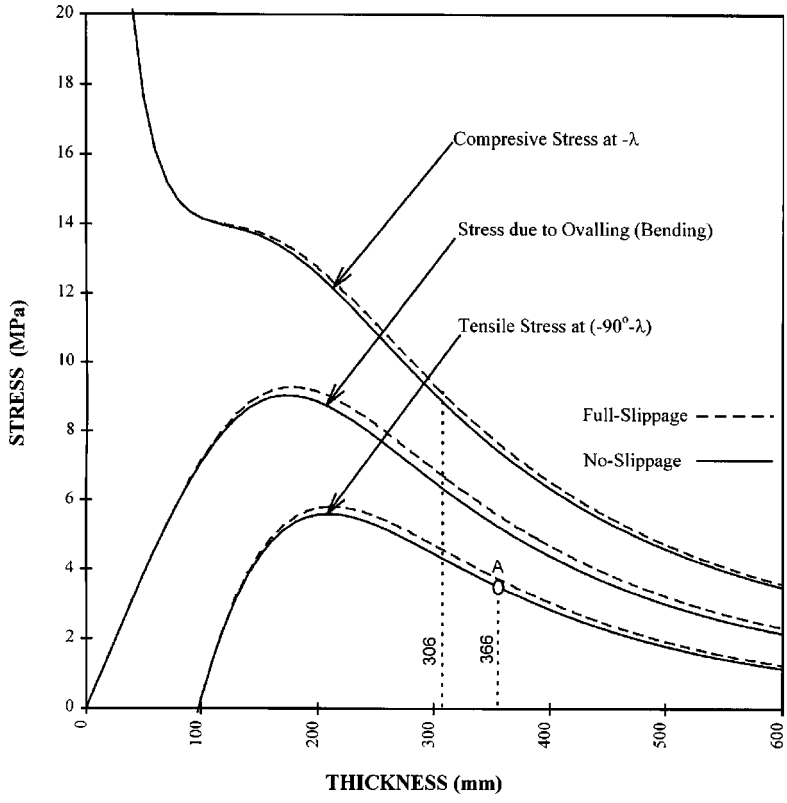

Figure 8. Stresses at inner fibres of concrete lining

value results in decreasing this critical stress. This latter decreasing of the critical stress is due to the increasing strong soil–lining interaction which takes place.

CONCLUDING REMARKS

The unified treatment of kinematic soil–lining interactions produced by (1) relaxation of *in situ* soil stresses near a lining following its installation, (2) overburden pressure applied to the soil surface, and (3) free-field soil response resulting from an earthquake, as presented herein, provides simple formulas for the calculation of lining deformations, forces, and corresponding stresses. These response quantities as produced by the relaxation of *in situ* soil stresses are significantly reduced from those produced by the 'equivalent' overburden pressure loading, $p = \gamma_s H_s$ thus, distinctly different solutions should be used for these two loading cases to avoid unnecessary conservatism in design.

The separate solutions obtained for the cases of full slippage and no slippage at the soil/lining interface during the occurrence of shear-type deformations indicated that full slippage has only a small effect on the shear and bending moments in the lining, but does reduce the maximum axial force by approximately 50 per cent. However, since the axial force produced by the dilatational-type deformation is much greater than the maximum axial force produced by the shear-type deformation, this 50 per cent reduction has little effect on the combined axial force due to both types of deformation. Consistent with this observation, slippage has little effect on the maximum combined normal stresses in the lining as produced by *in situ* stress relaxation and seismic free-field soil response.

It should be emphasized that the analytical procedure developed herein for determining lining stresses following installation is based on the assumption of perfect construction methods, i.e. the lining is placed in position in a circular stress-free state and grouting outside the lining completely fills all voids present. Since a perfect installation of this type cannot be achieved, the stress-state of linings as actually installed and the deficiencies which can occur in grouting should be taken into consideration in the design process. As pointed out by Kuesel,[7] the steel rings installed in the BART tunnels were subjected to considerable ovalling due to elastic flexure and working of the joints under their own dead weight and additional distortions were introduced as the linings were bolted together. Even though uncertainties exist regarding the stress state of linings during and following construction, evaluation of stress states under assumed ideal conditions, using the procedures developed herein, provides a sound starting point, the results of which can then be adjusted using engineering judgement as deemed appropriate.

Under extreme seismic conditions, the lining cross-section may deform significantly into the inelastic range. Such deformations should be controlled so as to force them to occur in the interior regions of the lining segments, not in the circumferential joints. Under moderate seismic conditions, the lining should be designed to remain elastic; in which case, the analytical procedures developed herein can be used to assess performance.[8,9]

REFERENCES

1. J. Q. Burns and R. M. Richard, 'Attenuation of stresses for buried cylinders', *Proc. Symp. on Soil–Structure Interaction*, *University of Arizona*, Engineering Research Laboratory, Tucson, AZ, September, 1964.
2. R. B. Peck, A. J. Hendron Jr. and B. Mohraz, 'State of the art of soft-ground tunneling', *Proc. RETC*, Vol. 1, 1972.
3. H. H. Einstein and C. W. Schwartz, 'Simplified analysis for tunnel supports', *J. Geotech. Engineering Div. ASCE*, **GT4**, 499–518 (April 1979).
4. J. L. Merritt, J. E. Monsees and A. J. Hendron, 'Seismic design of underground structures', *Proc. RETC*, Vol. 1, 1985.
5. J.-N. Wang, *Seismic Design of Tunnels*, Monograph 7, Parsons Brinkerhoff Quade & Douglas, June 1993.
6. S. Timoshenko and J. N. Goodier, *Theory of Elasticity*, 2nd edn, McGraw-Hill, New York, 1951.
7. T. R. Kuesel, 'Soft ground tunnels for the BART project', *Proc. RETC*, Vol. 1, 1972.
8. C. L. Wu and J. Penzien, 'Seismic design of MUNI metro turnback project', *Proc. 5th U.S. National Conf. on Earthquake Engineering*, Vol. IV, 1994.
9. C. L. Wu and J. Penzien, 'Stress analysis and design of tunnel linings'. *Proc. RETC*, Las Vegas, NV, June 1997.

